Full-Wave Analysis and Design of a New Double-Sided Branch-Line Coupler and Its Complementary Structure

Chung-Yi Lee, *Student Member, IEEE,* and Tatsuo Itoh, *Fellow, IEEE*

Abstract— **A new double-sided branch-line coupler using microstrip lines as input/output lines and slotlines as branches is analyzed and designed. The even-odd mode theory is first used to analyze the ideally simplified circuit model and to find out the preliminary circuit dimensions. Based on these dimensions, the full-wave spectral domain approach (SDA) is employed to accurately simulate the circuit performance. By the formulation of the exact Green's function in the spectral domain, the effects of surface wave and radiation phenomena are accurately accounted for. Experimental data agree very well with the SDA simulation results. It is found that the even-odd mode theory which neglects discontinuities between lines is not enough to design a coupler. The SDA code can then be used to accurately simulate and optimize the circuit performance. The complementary structure with slotlines as input/output lines and microstrip lines as branches is also investigated both theoretically and experimentally. It is noticed that the radiation and leakage from the two double-ended branches for all structures will deteriorate the circuit performance.**

I. Introduction

THE BRANCH-LINE coupler has wide applications, such as 90° power combiners, power dividers, balanced amplifiers, and balanced mixers. For the conventional coupler using microstrip lines, the junctions between the input/output lines and the quarter-wavelength sections are all in parallel connections and on the same side of the substrate. Recently, some efforts had been made to implement this type of circuit on the monolithic microwave integrated circuit (MMIC) [1]–[2], to overcome the impedance problems of symmetrical and asymmetrical couplers [3]–[4], and to include the effect of finite metallization thickness [5]. A uniplanar branch-line coupler which uses only one side of metallization was established by utilizing a coupled rectangular slotline ring [6]. Other circuits using the features of double-sided microwave integrated circuits (double-sided MIC's) [7], which effectively utilize various kinds of transmission lines on both sides of a substrate, were also investigated in the past. The microstrip-slot coupler was originally proposed by deRonde [8], and some studies had been done to analyze and improve the circuit performance [9]–[12]. The complementary structure to the work done by Hoffman and Siegl [12] are realized on the fin-line [13]. Moreover, the slot-coupled directional coupler was developed in [14]. Nevertheless, all the previous works used the even-odd mode theory only to analyze circuit performance. No full-wave analysis has been used to accurately account for the discontinuities between lines. For the design of microwave and millimeter-wave integrated circuits (MIMIC's), a proper designing tool which includes all physical effects is needed to avoid the trial and error processes.

Fig. 1 shows the proposed new double-sided branch-line coupler, hereafter referred to as structure A, which employs the coupling mechanism between transmission lines on different sides of the substrate. The microstrip lines are used as the input and output lines, while slotlines which are built on the ground plane of and orthogonal to microstrip lines are used as branches. The distance between two microstrip or slot lines is quarter-wavelength, and all shorted slotline stubs are also about quarter-wavelength. In this configuration, the junction between microstrip and slot lines are series connections in the simplified circuit model shown in Fig. 2. Based on the even-odd mode theory, it is possible to make two different 3-dB branch-line couplers by suitably choosing the values of Z_m and Z_s. The spectral domain approach (SDA), which has been used successfully to analyze discontinuities of planar circuits [15]–[18], is utilized to simulate this new type of coupler and to check the limitations of the even-odd theory on the circuit design. To the best of the authors' knowledge, this is the first time that a full-wave analysis is applied to the coupler design. Experimental data of both single- and double-layered structures are shown to validate the accuracy of the SDA simulation code. The effects of the dielectric constant and the substrate thickness are studied. It is found that the circuit performance will deteriorate and deviate from the designed frequency under some circumstances, if one only uses the circuit theory which neglects the discontinuities between lines to design a coupler. The SDA analysis code can then be used to accurately simulate and optimize the circuit performance.

The complementary circuit of structure A with microstrip and slot lines switching their positions in Fig. 1(a) is also investigated and will be referred to as structure B. Fig. 3 shows the simplified circuit model of structure B. As it can be seen, the junctions between lines are parallel connections instead of the series ones shown in Fig. 2. This is due to the difference in end discontinuities of branches. The open-ended microstrip lines are used in structure B, while the short-ended slotlines are used in structure A. In Section II, the theoretical formulation of both the even-odd mode theory

Manuscript received September 6, 1994; revised April 24, 1995. This work was supported by TRW MICRO.

The authors are with the Department of Electrical Engineering, University of California, Los Angeles, Los Angeles, CA 90095 USA.

IEEE Log Number 9412683.

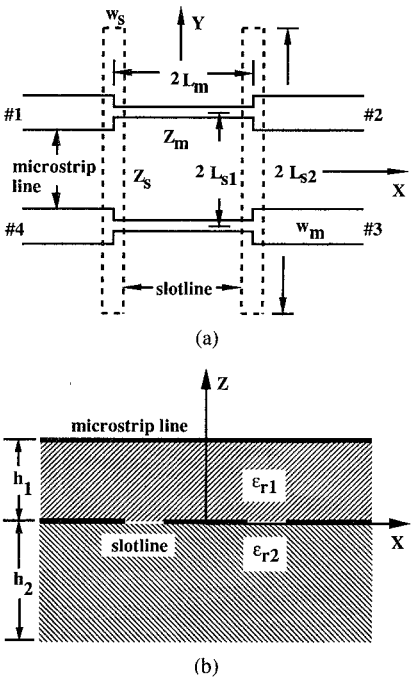

Fig. 1. A series type branch-line coupler of structure A. (a) Top view. (b) Cross section.

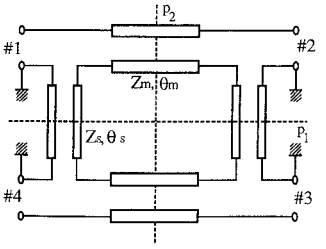

Fig. 2. Simplified four-port network of structure A.

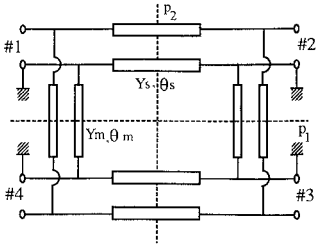

Fig. 3. Simplified four-port network of structure B.

and full-wave SDA for structure A will be discussed. The analytical procedures for structure B are similar, hence only the theoretical and experimental results will be shown and discussed.

II. Analytical Formulation

A. Even-Odd Mode Theory [12], [19]

Fig. 2 shows the simplified four-port network of structure A with two symmetrical planes P_1 and P_2, and θ_m and θ_s are 90° representing the electrical length of quarter-wavelength sections. From the even-odd mode theory, the scattering parameters of Fig. 2 can be deduced as

$$S_{11} = \frac{-1 + (Z_m^2 - Z_s^2)^2}{\Delta} \tag{1}$$

$$S_{21} = \frac{-2jZ_m(1 + Z_m^2 - Z_s^2)}{\Delta} \tag{2}$$

$$S_{31} = \frac{4Z_m Z_s}{\Delta} \tag{3}$$

$$S_{41} = \frac{-2jZ_s(1 - Z_m^2 + Z_s^2)}{\Delta} \tag{4}$$

where $\Delta = (1 + (Z_m + Z_s)^2)(1 + (Z_m - Z_s)^2)$ and Z_m and Z_s are the normalized characteristic impedance of quarter-wavelength sections of the microstrip line and the slotline, respectively. According to (1)–(4), there are two possible matching conditions ($S_{11} = 0$), i.e., there are two available coupling mechanism as described below.

Type I: $Z_m^2 - Z_s^2 = -1$ The scattering parameters under such a condition are

$$S_{11} = S_{21} = 0, \quad S_{41}/S_{31} = 1/jZ_m. \tag{5}$$

A balanced branch-line coupler can be realized by choosing $Z_m = 1$ and $Z_s = \sqrt{2}$. Under this arrangement, port 2 is the isolation port, while the signal output at ports 3 and 4 are equal in amplitude and in phase quadrature. This feature of power distributions is different from the conventional branch-line and microstrip-slot couplers [8]–[12].

Type II: $Z_m^2 - Z_s^2 = 1$ The scattering parameters under such a condition are

$$S_{11} = S_{41} = 0, \quad S_{21}/S_{31} = 1/jZ_s. \tag{6}$$

Similarly, an equal power coupler can be realized by choosing $Z_m = \sqrt{2}$ and $Z_s = 1$. Under such a condition, port 4 is the isolation port, while the signal output at ports 2 and 3 are equal in amplitude and in phase quadrature.

Nevertheless, considering the different impedance properties between microstrip and slot lines, it is more suitable to make a circuit with a higher slotline characteristic impedance than that of the microstrip line. Therefore, we will choose the type I coupler to fulfill our structure.

B. Spectral Domain Approach [18], [20]

The method consists of two main parts: eigenvalue formulation and scattering parameters calculation. The first part is used to determine the propagation constant and characteristic impedance of an infinitely long microstrip line. This information will be used in the second part to form the characteristics of guided waves on the input/output ports.

To compute the scattering parameters of the coupled 4-port circuit, a modified version of the deterministic spectral domain method is applied. The multilayered Green's function is derived first to account for all physical phenomena including surface wave and radiation effects. Then the coupling structure of Fig. 1 is divided into two regions: the uniform region where only the dominant mode is propagating, and the coupling region where all possible modes exist. The arrangement of basis functions for the type I balanced coupler ($Z_m = 1$ and $Z_s = \sqrt{2}$) is shown in Fig. 4. Although Fig. 1(a) is a general

coupler structure, both transverse and longitudinal currents and fields should be used to accurately include the effects of step discontinuities. For the present type I case, there are no width changes on microstrip lines. For simplicity, we only use the dominant electric current and field which are good enough to analyze the coupler as discussed in [15] and [16]. Assume that an incident current originated from $x = -\infty$ of port 1. Then the longitudinal current distributions on ports 1–4 in the uniform region can be expressed as

$$J_u^1(x,y) = \sum_i a_i \cdot \phi_i^m(y - L_{s1}) \cdot (e^{-j\alpha_m(x+L_m)} - \Gamma e^{j\alpha_m(x+L_m)}) \quad (7)$$

$$J_u^2(x,y) = \sum_i b_i \cdot \phi_i^m(y - L_{s1}) \cdot T_2 \cdot e^{-j\alpha_m(x-L_m)} \quad (8)$$

$$J_u^3(x,y) = \sum_i c_i \cdot \phi_i^m(y + L_{s1}) \cdot T_3 \cdot e^{j\alpha_m(x+L_m)} \quad (9)$$

$$J_u^4(x,y) = \sum_i d_i \cdot \phi_i^m(y + L_{s1}) \cdot T_4 \cdot e^{j\alpha_m(x+L_m)} \quad (10)$$

where Γ and T_i are the unknown complex reflection coefficient on port 1 and transmission coefficients on other ports, $\phi_i^m(y)$ is the transverse dependence basis functions used in the eigenvalue calculations. α_m is the phase constant and a_i to d_i are the current coefficients of input/output microstrip lines. These quantities are solved from the first part. In the coupling region, the strip currents and slot fields are assumed to be the superposition of the current in the uniform region and a perturbed current/field which represents the higher order modes variation. On the input/output lines, they can be expressed as

$$J_c^1(x,y) = J_u^1(x,y) + \sum_j \sum_k a'_{jk} \cdot \phi_j^{m'}(y - L_{s1}) \cdot \varphi_k^{m'}(x + L_m) \quad (11)$$

$$J_c^2(x,y) = J_u^2(x,y) + \sum_j \sum_k b'_{jk} \cdot \phi_j^{m'}(y - L_{s1}) \cdot \varphi_k^{m'}(x - L_m) \quad (12)$$

$$J_c^3(x,y) = J_u^3(x,y) + \sum_j \sum_k c'_{jk} \cdot \phi_j^{m'}(y + L_{s1}) \cdot \varphi_k^{m'}(x - L_m) \quad (13)$$

$$J_c^4(x,y) = J_u^4(x,y) + \sum_j \sum_k d'_{jk} \cdot \phi_j^{m'}(y + L_{s1}) \cdot \varphi_k^{m'}(x + L_m) \quad (14)$$

where a'_{jk} to d'_{jk} represent the complex amplitudes of higher order modes. These higher order modes should disappear as the observation point is far away from the discontinuities. In other words, when disturbed J_c^i's approach the ends of the coupling region, they should be degenerated to dominant J_u^i's in uniform regions. On the quarter-wavelength microstrip sections, current distributions are expressed as

$$J_c^{12}(x,y) = \sum_l \sum_m e'_{lm} \cdot \phi_l^{m'}(y - L_{s1}) \cdot \varphi_m^{m'}(x - L_m) \quad (15)$$

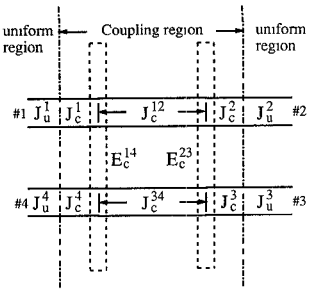

Fig. 4. Arrangement of basis functions for the type I balanced coupler of structure A.

$$J_c^{34}(x,y) = \sum_l \sum_m f'_{lm} \cdot \phi_l^{m'}(y + L_{s1}) \cdot \varphi_m^{m'}(x - L_m). \quad (16)$$

The asymmetrical basis functions are placed at both ends of quarter-wavelength sections to ensure that currents are continuous between the junctions of microstrip lines. On the two shorted slotlines, the transverse aperture fields are assumed to be

$$E_c^{14}(x,y) = \sum_p \sum_q g'_{pq} \cdot \phi_p^{s'}(x + L_m) \cdot \varphi_q^{s'}(y - L_{s2}) \quad (17)$$

$$E_c^{23}(x,y) = \sum_p \sum_q h'_{pq} \cdot \phi_p^{s'}(x - L_m) \cdot \varphi_q^{s'}(y - L_{s2}) \quad (18)$$

where $\varphi^{m'}(x), \phi^{s'}(x), \phi^{m'}(y)$ and $\varphi^{s'}(y)$ are the x and y dependence of basis functions. In general, the two-directional and subsectional basis functions should be used in both x and y dependence to accommodate possible high order variation and also to add flexibility to the structure configuration. Nevertheless, the entire domain basis functions for $\phi^{s'}(x)$ and $\phi^{m'}(y)$ can be used to satisfy edge conditions and to provide fast convergence if the type I balanced coupler is analyzed. For $\varphi^{m'}(x)$ and $\varphi^{s'}(y)$, we use the rooftop basis functions for all cases discussed in this paper.

The method of moments is then applied to generate a set of linear equations in which reflection, transmission and perturbed current/field coefficients are unknown. From the solutions of these unknowns, the coupling mechanism of the branch-line coupler is completely determined. By using the transmission line theory, we can easily extract the scattering parameters from the reflection and transmission coefficients defined in (7)–(10). We can also calculate total circuit loss due to the combination of surface-wave and space-wave radiation by computing [15]

$$\text{Loss} = 1 - \sum_{i=1}^{4} |S_{i1}|^2. \quad (19)$$

III. Results

Case A. Single-Layered Substrate ($h1 \neq 0, h2 = 0$) of Structure A

In order to avoid the large width ratio between microstrip and slot lines, the 70 Ω microstrip line and 99 Ω slotline are

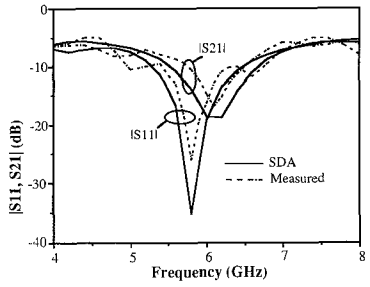

Fig. 5. Magnitude of scattering parameters of case A.

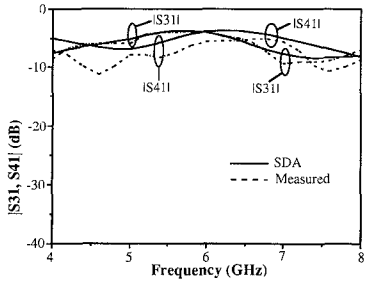

Fig. 6. Magnitude of scattering parameters of case A.

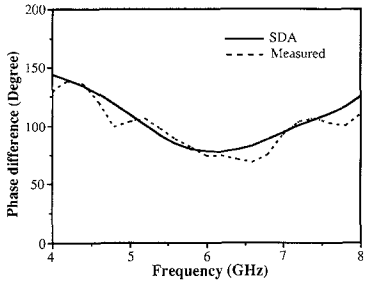

Fig. 7. Phase difference between ports 3 and 4 of case A.

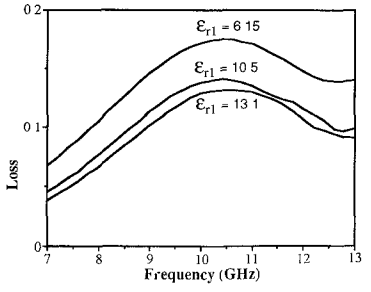

Fig. 8. Total circuit loss for the different substrate dielectric constant of case A.

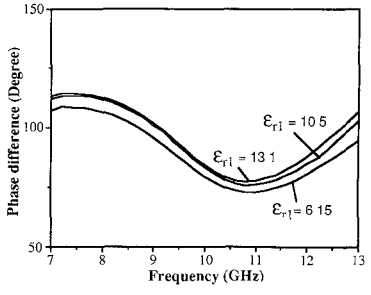

Fig. 9. Phase difference for the different substrate dielectric constant of case A.

chosen to design the new branch-line coupler with one-layered substrate only. According to (5) and the eigenvalue analysis of both uniform microstrip and slot lines, a series type branch-line coupler of structure A was designed and built on an RT/Duroid 6010 ($\varepsilon_{r1} = 10.5$) substrate with the following dimensions: a) substrate thickness $h_1 = 25$ mil, b) microstrip line width $w_m =$ 10 mil, c) slotline width $w_s = 22$ mil, d) quarter-wavelength microstrip line length $2L_m = 189$ mil, e) quarter-wavelength slotline length $2L_{s1} = 274$ mil, f) total slotline length $2L_{s2} =$ 816 mil. In our analysis, the substrate is lossless with infinite extent and the conductor loss is omitted. Figs. 5–7 compare the SDA simulated and measured data. The simulated equal power level is about $-$ 4 dB and phase difference between ports 3 and 4 is 77.5° at 6 GHz. The 1 dB bandwidth is about 10%, the return loss and isolation are better than 15 dB in this range. It is found that both the power level and phase difference are different from the ideal coupler, i.e., $-$ 3 dB output power and phase quadrature. The reason for this deviation is considered mainly coming from the radiation and leakage from the two slotlines which act as antennas. These effects are accurately accounted for in the full-wave analysis. These phenomena could also be observed in [6] which used rectangular slot ring as the coupling mechanism and phase difference is maintained at $83° \pm 3°$ over a certain bandwidth. As it can be seen, the SDA code accurately predict the dip positions of the $|S_{11}|$ and $|S_{21}|$. The measured equal power level is about $-$ 5.66 dB at 6.5 GHz, the phase difference is 79° at 6 GHz, and 1 dB bandwidth is 8%. This phase value is well predicted at the center frequency. The measured $|S_{31}|$ matches the simulation data best. The discrepancies from simulation are partly due to the fabrication tolerances and loss comes from the conductor and transitions between lines.

Fig. 8 shows the total circuit loss for different substrate dielectric constants, while the characteristic impedance is kept unchanged. It can be seen that the loss can be reduced by increasing the substrate dielectric constant. All the loss peaks occur around the center frequency 10 GHz where most of the power couples from microstrip to slot lines due to the shorted slotline stubs. Fig. 9 shows that the phase difference can approach the ideal 90° by increasing ε_{r1}. Fig. 10 is the phase differences for different substrate thickness. It can be seen that the thicker the substrate is, the larger the variation. The reason is that the characteristic impedance is more dispersive if a thicker substrate is used. It is also found that the circuit performance will deteriorate and shift more from our expectation of the even-odd mode theory, if the thicker substrate is used. This means that the circuit theory is no longer a good enough design tool. A proper analysis technique, e.g., the SDA code must be utilized to simulate and optimize the performance. In the next subsection, a two-layered substrate case, we will present the need and procedures of optimization by using the SDA code.

Case B. Double-Layered Substrate ($h1 \neq 0, h2 \neq 0$) of Structure A

In order to realize this new coupler to a conventional 50 Ω microstrip line, one has to reduce the impedance of the slotline

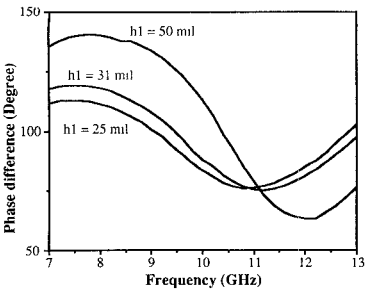

Fig. 10. Phase difference for the different substrate thickness of case A.

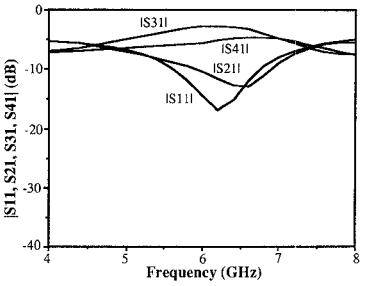

Fig. 11. Simulated scattering parameters before optimization of case B.

with the width ratio kept in a reasonable range. Here we use a double-layered slotline to reduce the slotline impedance so that the comparable line widths of microstrip and slot lines can be obtained. The even-odd mode theory is used first to synthesize the 50 Ω microstrip line and 70.7 Ω slotline coupler. Based on these dimensions, the SDA code is used to simulate its performance. The result is shown in Fig. 11 which is a totally unacceptable result. A suitable analysis method which includes all the physical effects should be used to optimize the circuit performance. The SDA code provides the good potential for doing this work. First, we adjust the slotline width such that the equal power point is around the designed frequency 6 GHz. Then by varying the length of shorted slotline stubs, the phase difference can be changed. The circuit dimensions after optimization are: a) dielectric constant $\varepsilon_{r1} = \varepsilon_{r2} = 10.5$, b) substrate thickness $h_1 = h_2 = 25$ mil, c) microstrip line width $w_m = 22.5$ mil, d) slotline width $w_s = 22$ mil, e) quarter-wavelength microstrip line length $2L_m = 184$ mil, f) quarter-wavelength slotline length $2L_{s1} = 200$ mil, g) total slotline length $2L_{s2} = 580$ mil. Fig. 12 is the simulated amplitudes of scattering parameters after optimization, the equal power level is -3.54 dB, and the power difference between ports 3 and 4 is within 1 dB for frequencies less then 6.35 GHz. Figs. 13–15 show the comparison between the simulated and measured data. The dips of $|S_{11}|$ and $|S_{21}|$ are again accurately predicted. The measured equal power level is $-$ 4.3 dB at 6.1 GHz, and 1 dB bandwidth is about 20%. The phase difference curves match very well around the designed frequency 6 GHz. As it can be seen, these theoretical and experimental data in Figs. 13-15 agree better than those of case A in Figs. 5–7. The main difference is that there is no quarter-wavelength transformer in the present case of 50 Ω microstrip lines. Fig. 16 shows that the circuit loss is less than 10%. This is why the power level and phase difference in Figs. 12 and 15 are closer to an ideal coupler compared with

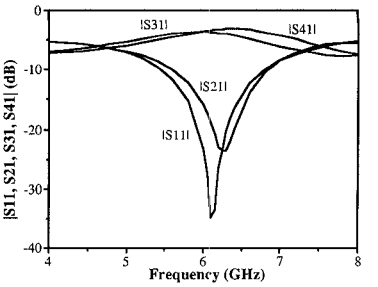

Fig. 12. Simulated scattering parameters after optimization of case B.

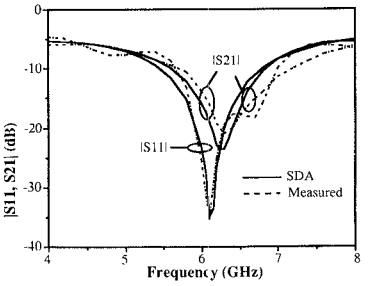

Fig. 13. Magnitude of scattering parameters of case B.

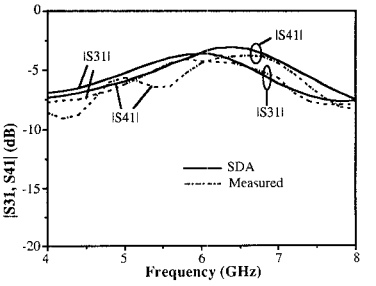

Fig. 14. Magnitude of scattering parameters of case B.

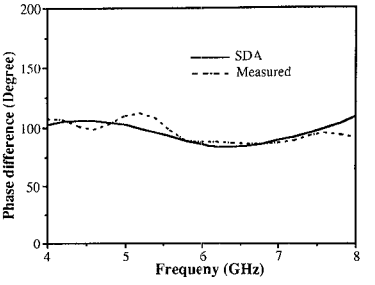

Fig. 15. Phase difference between ports 3 and 4 of case B.

the case of a single-layered substrate. However, this loss might still deteriorates the circuit performance.

Case C. Single-Layered Substrate ($h_1 \neq 0, h_2 = 0$) of Structure B

There are two available power distributions on output ports after the even-odd mode analysis for structure B. We choose the normalized admittance $Y_s = 1$ and $Y_m = \sqrt{2}$ to realize the 3-dB coupler. It should be noticed that there are no step discontinuities on the slotlines in our design. This will simplify the formulation processes as stated in Section II, since only the dominant basis functions are adequate to simulate the circuit.

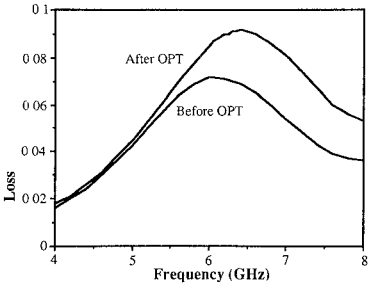

Fig. 16. Total circuit loss of case B.

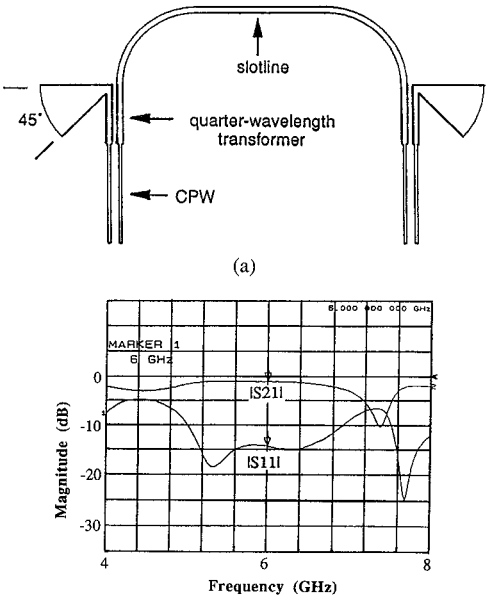

Fig. 17. CPW-to-slotline transition with quarter-wavelength matching sections. (a) Back-to-back circuit layout. (b) Measured performance.

Under this arrangement, port 2 is the isolation port, while the signal output at ports 3 and 4 are equal in amplitude and in phase quadrature. The phase of port 4 leads that of port 3 by 90°. This feature is different from that of structure A where the phase of port 3 leads that of port 4 by 90°.

The coplanar waveguide (CPW) is employed as the intermediate stage between slotlines and the measurement system HP8720A. The CPW-to-slotline transition is first studied experimentally based on the circuit topology proposed in [6]. To accommodate the complete circuit, the transition using a CPW short and a slotline radial stub is chosen. In addition, a quarter-wavelength CPW transformer is used to match the impedance difference between CPW and slotline. Several circuits of different spanned angles of radial stubs are tested. The back-to-back transition which is suitable for our applications is shown in Fig. 17(a). Fig. 17(b) is its measured performance. The insertion loss is less than 1.3 dB in the 5.0–6.6 GHz. Therefore, the interested coupler performance will be confined in this frequency range.

As in structure A, the spectral domain code is used to simulate and optimize the circuit performance which was designed first by using the even-odd mode analysis. The optimized branch-line coupler was built on an RT/Duroid 6010

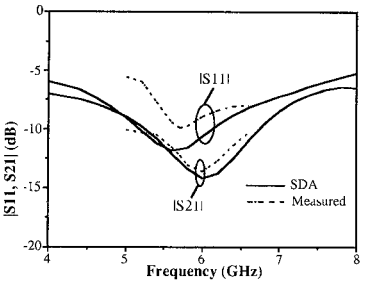

Fig. 18. Magnitude of scattering parameters of case C.

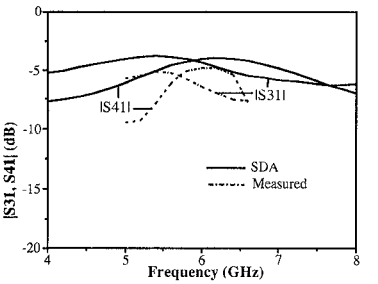

Fig. 19. Magnitude of scattering parameters of case C.

($\varepsilon_{r1} = 10.5$) substrate with the following dimensions: a) substrate thickness $h_1 = 25$ mil, b) microstrip line width $w_m = 18$ mil, c) slotline width $w_s = 22$ mil, d) quarter-wavelength slotline length $2L_s = 271$ mil, e) quarter-wavelength microstrip line length $2L_{m1} = 186$ mil, f) total microstrip line length $2L_{m2} = 590$ mil. In this analysis, all the substrate and conductor losses are excluded. Figs. 18 and 19 show the simulated amplitudes of scattering parameters. In addition the measured data in the 5.0–6.6 GHz range are also shown. In simulation, the equal power level is about −4.1 dB at 5.9 GHz and 1 dB bandwidth is about 15%. As it can be seen, the measured dip positions of $|S_{11}|$ and $|S_{21}|$ and the equal power frequency are well predicted by the SDA code. The measured power level of $|S_{21}|$ agrees well with the simulation and the equal power level is −5.5 dB at 5.7 GHz. Fig. 20 shows the phase difference between ports 3 and 4 and the total circuit loss. The simulated phase value is 97.7° and measured one is 94.7° at 6 GHz. There is still certain amount of loss which makes the circuit deviating from an ideal case, i.e., −3 dB output power and phase quadrature. In addition to the surface wave, the loss comes from the radiation of the two open-ended microstrip lines which act as dipole antennas. These effects are exactly accounted for in the spectral domain Green's function. The deviation of measured power levels from simulation comes partly from the CPW-to-slotline transitions, circuit misalignment, and the conductor loss.

IV. Conclusion

The study of electromagnetic characteristics between lines on different layers of a circuit is an important step in multilayered MIMIC's. It provides us one more degree of freedom to design circuits. Two new double-sided branch-line couplers, using electromagnetic coupling mechanism, with series or parallel junctions between lines are developed. Both the circuit

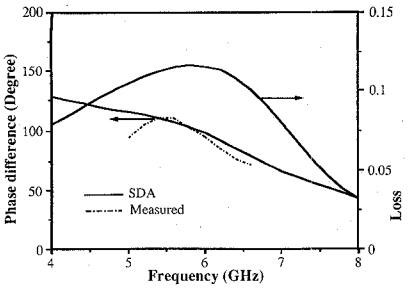

Fig. 20. Phase difference between ports 3 and 4 and total circuit loss of case C.

theory, which neglects discontinuities between lines, and the spectral domain approach, which includes all the physical phenomena, are used to analyze and design these circuits. Experimental data agree well with those of simulation by using the SDA code. It is shown that the circuit theory is not enough to design a circuit and an accurate electromagnetic field technique should be used to verify the circuit performance. The SDA code can accurately predict the circuit performance. More importantly, it can be used to optimize the circuit. It is also noticed that the radiation and leakage from the two double-ended branches for all structures will deteriorate the circuit performance.

ACKNOWLEDGMENT

The authors would like to thank M. Christianson at the center of High Frequency Electronics of University of California at Los Angeles for assembly of circuits.

REFERENCES

[1] T. Hirota, Y. Minakawa, and M. Muraguchi, "Reduced-size branch-line and rat-race hybrids for uniplanar MMIC's," *IEEE Trans. Microwave Theory Tech.*, vol. 38, pp. 270–275, Mar. 1990.

[2] I. Toyoda, T. Hirota, and T. Tokumitsu, "Multilayer MMIC branch-line coupler and broad-side coupler," in *IEEE MTT-S Int. Microwave Symp. Dig.*, 1992, pp. 79–82.

[3] H. Ashoka, "Practical realization of difficult microstrip line hybrid couplers and power dividers," in *IEEE MTT-S Int. Microwave Symp. Dig.*, 1992, pp. 273–276.

[4] J. W. Gipprich, " A new class of branch-line directional couplers," in *IEEE MTT-S Int. Microwave Symp. Dig.*, 1993, pp. 589–592.

[5] F. Alessandrî, M. Mongiardô, R. Sorrentinô, and J. Uher, "Analysis of branch line coupler in suspended stripline with finite metallization thickness," in *IEEE MTT-s Int. Microwave Symp. Dig.*, 1993, pp. 1089–1092.

[6] C. H. Ho, L. Fan, and K. Chang, "Broad-band uniplanar hybrid-ring and branch-line couplers," *IEEE Trans. Microwave Theory Tech.*, vol. 41, pp. 2116–2125, Dec. 1993.

[7] M. Aikawa and H. Ogawa, "Double-sided MIC's and their applications," *IEEE Trans. Microwave Theory Tech.*, vol. 37, pp. 406–413, Feb. 1989.

[8] F. C. deRonde, "A new class of microstrip directional coupler," in *IEEE MTT-S Int. Microwave Symp. Dig.*, 1970, pp. 184–186.

[9] J. A. Garcia, "A wide-band quadrature hybrid coupler," *IEEE Trans. Microwave Theory Tech.*, pp. 660–661, July 1971.

[10] B. Schiek, "Hybrid branchline couplers—A useful new class of directional couplers," *IEEE Trans. Microwave Theory Tech.*, vol. MTT-22, pp. 864–869, Oct. 1974.

[11] B. Schiek and J. Köhler, "Improving the isolation of 3-dB couplers in microstrip-slotline technique," *IEEE Trans. Microwave Theory Tech.*, vol. MTT-26, pp. 5–7, Jan. 1978.

[12] R. Hoffmann and J. Siegl, "Microstrip-slot coupler design," *IEEE Trans. Microwave Theory Tech., Part I and II*, vol. MTT-30, pp. 1205–1216, Aug. 1982.

[13] M. Schoenberger, A. Biswas, A. Mortazawi, and V. K. Tripathi, "Coupled slot-strip coupler in finline," *IEEE MTT-S Int. Microwave Symp. Dig.*, 1991, pp. 751–753.

[14] T. Tanaka, K. Tsunoda, and M. Aikawa, "New slot-coupled directional couplers between double-sided substrate microstrip lines, and their applications," in *IEEE MTT-S Int. Microwave Symp. Dig.*, 1988, pp. 579–582.

[15] R. W. Jackson and D. M. Pozar, "Full-wave analysis of microstrip open-end and gap discontinuities," *IEEE Trans. Microwave Theory Tech.*, vol. MTT-33, pp. 1036–1042, Oct. 1985.

[16] H. Y. Yang and N. G. Alexópoulos, "A dynamic model for microstrip-slotline transition and related structures," *IEEE Trans. Microwave Theory Tech.*, vol. 36, pp. 286–293, Feb. 1988.

[17] Y. M. M. Antar, A K. Bhattcharyya, and A. Ittipiboon, "Microstripline-slotline transition analysis using the spectral domain technique," *IEEE Trans. Microwave Theory Tech.*, vol. 40, pp. 515–523, Mar. 1992.

[18] A. Tran and T. Itoh, "Full-wave modeling of coplanar waveguide discontinuities with finite conductor thickness," *IEEE Trans. Microwave Theory Tech.*, vol. 41, pp. 1611–1615, Sept. 1993.

[19] R. Levy, "Directional couplers," in *Advances in Microwaves*, L. Young, Ed., vol. 1. New York: Academic, 1966.

[20] T. Itoh, *Numerical Techniques for Microwave and Millimeter-Wave Passive Structures*. New York: Wiley, 1989.

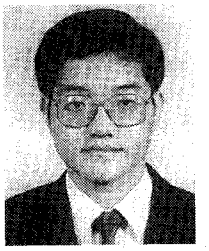

Chung-Yi Lee (S'94) was born in Hualien, Taiwan, on April 7, 1965. He received the B.S. degree from Chun Yuan University, Chunli, Taiwan, the M.S. degree from the National Chiao Tung University, Hsinchu, Taiwan, and the Ph.D. degree from the University of California, Los Angeles, in 1987, 1989, and 1995, respectively.

From 1991 to 1992, he was on the faculty at the Chinese Junior College of Marine Technology, Taipei, Taiwan. From 1992–1995, he was a Graduate Research Student Researcher with the University of California, Los Angeles, where he is now a Postdoctoral Fellow. His research interests include wireless communications, microwave and millimeter-wave integrated circuits, antenna designs, and the development of electromagnetic simulation tools.

Tatsuo Itoh (S'69–M'69–SM'74–F'82), for a photograph and biography, see this issue, p. 1874.